2023 62nd IEEE Conference on Decision and Control (CDC)
December 13-15, 2023. Marina Bay Sands, Singapore

# Predator-Prey Interactions through Heterogeneous Coverage Control Using Reaction-Diffusion Processes

Ruoyu Lin† and Magnus Egerstedt†

***Abstract*— A predator-prey interaction scheme based on a heterogeneous cooperative control strategy driven by reaction-diffusion processes is investigated in this paper, where the heterogeneity is understood along five modalities in terms of the dynamics of predator and prey. The predators are modeled as individual agents whereas the prey are modeled as space-time dependent densities. A decentralized coverage controller for predators with heterogeneous mobility, encoded by multiplicatively weighted Voronoi cells, is derived so that the predators can optimally react to the time-varying prey distributions. The predator-prey interaction scheme can be adopted in diverse application scenarios. An experiment of deploying a multi-robot system across a two-dimensional domain pictorially representing a forest in which ideally modeled wildfires need to be put out demonstrates the efficacy of the proposed scheme.**

## I. Introduction

Cooperation and collaboration are critical survival strategies in nature. Lions and dolphins form predator fronts charging through the aggregation of prey [1], which is an example of cooperation. Langur monkeys help chital deers obtain food from vegetation to which the chital deers have no access and they both react to each other's alarm of potential predators [2], which is an example of collaboration. A number of those strategies have served as sources of inspiration for multi-robot system design [3]–[6], where, as discussed in [7], cooperation considers that agents share goals and leverage others' help to improve task performance as a whole team, e.g., [3], and collaboration considers that agents leverage complementary capabilities due to specific task requirements and inherent agent constraints, e.g., [8]. In particular, some pursuit–evasion robotic tasks, such as protecting an area from intruders, take advantage of the cooperative mobility strategies that predators utilize for hunting prey [9].

A typical approach to solving pursuit–evasion (predator hunting prey) problems optimally in terms of time is through the Hamilton-Jacobi-Isaacs equation, corresponding to a differential game, e.g., [10]–[12]. However, many differential game-based approaches for solving pursuit–evasion problems do not scale well due to high computational complexity. A decentralized Voronoi tessellation-based strategy for multiple pursuers capturing one evader in a 2-dimensional domain of interest is proposed in [13]. Subsequently, [14] extends the work in [13] to the case of higher dimensional bounded domains and multiple pursuers capturing multiple evaders, by providing a decentralized controller that drives each pursuer to the centroid of the bisector between the pursuer and its nearest evader. However, this strategy has a requirement that all the evaders and pursuers have the same maximum translational speeds, which cannot be extended to the heterogeneous case in a direct manner.

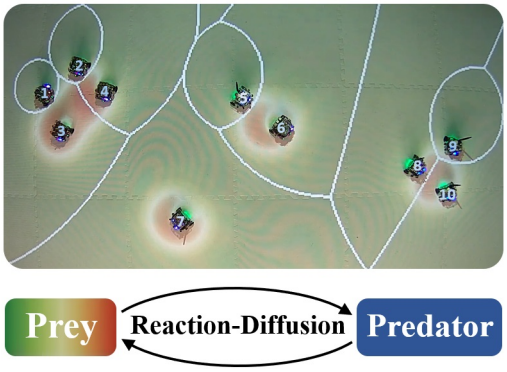


Fig. 1. Illustrating a team of predators, represented by differential-drive wheeled robots, each of which is in charge of a region of dominance enclosed by the white curves, "eating" the diffusing prey density with the red area representing high density and the green area representing low density. The prey's dynamics is affected by the predators' dynamics through a reaction-diffusion process, and conversely, the predators' dynamics is also driven by the prey's dynamics through their space-time dependent densities.

Instead of modeling the prey as individual evaders, we define space-time dependent densities to characterize the prey, as illustrated in Fig. 1. A similar idea of modeling the prey as density distributions is presented in [15], in which the prey refers to the food of the agents potentially targeted by other predators. However, the prey density at each point is only binary (i.e., either a positive constant or zero), which does not characterize a general dynamic food consumption model. Additionally, in [15], the method inspired by animals' foraging is introduced without consideration of heterogeneities among agents, and it is centralized since the agents are assumed to have access to information about all predators and food across the entire domain of interest.

The main novelty of this paper is to investigate a decentralized reaction-diffusion-based predator-prey interaction scheme considering heterogeneous predator and prey dynamics. The formulation is general and allows for diverse instantiations of the scheme, such as deployments of teams of mobile robots to clean up oil spills, e.g., [9], underwater robots for halobios monitoring, e.g., [16], and aerial robots to put out ideally modeled wildfires, e.g., [17]. Besides, the proposed scheme in this paper not only scales well due to its nature of decentralization, but also can handle multiple types

This work was supported by the U.S. Army Research Lab through ARL DCIST CRA W911NF-17-2-0181.

†Ruoyu Lin and Magnus Egerstedt are with the Department of Electrical Engineering and Computer Science, University of California, Irvine, CA 92697, USA. Email: {rlin10, magnus}@uci.edu

of tasks simultaneously. For example, Fig. 1 can depict that Robots 1, 2, 3, and 4 are putting out the wildfire represented by the density on the left of the domain, while Robots 8, 9, and 10 are arresting the arsonists represented by the density on the right. Meanwhile, Robots 5, 6, and 7 are searching and rescuing the injured represented by the two density distributions in the middle. During the process, some robots may switch their roles from firefighters to the injured searchers when they determine the rest of the firefighters are able to handle the mission of firefighting or the mission of injured searching needs more robots to help. Note that all these procedures happen automatically and in a decentralized manner benefiting from the formulation of the scheme that will be discussed in detail in the following sections.

The remainder of this paper is organized as follows: In Section II, a general heterogeneous prey model is introduced that can be applied to various scenarios by combining corresponding types of heterogeneous modalities defined in it. In Section III, we investigate a heterogeneous dynamics model for the predators that exponentially converges to and maintains a time-varying configuration that locally optimally covers the spatiotemporal prey density in a convex domain. In Section IV, a concrete application of the predator-prey interaction scheme is presented through an experiment, which demonstrates the effectiveness of the proposed scheme. Conclusions are presented in Section V.

## II. Heterogeneous Prey Model

Denote the convex domain of interest as $\mathcal{D} \subset \mathbb{R}^n$, the set of predators' indices as $\mathcal{N} = \{1, 2, \ldots, N\}$, where $n, N \in \mathbb{Z}_+$, the position of Predator $i$ as $p_i \in \mathcal{D}$, where $i \in \mathcal{N}$, and the vector of the $N$ predators' positions as $p = [p_1^T, p_2^T, \ldots, p_N^T]^T \in \mathbb{R}^{nN}$.

Inspired by [18] where the movement law of the prey density distribution is given by a reaction-diffusion equation based on the FitzHugh-Nagumo model [19] as

$$\frac{\partial \phi(q,t)}{\partial t} - \nu(\rho) \cdot \nabla^2 \phi(q,t) + \mu \cdot \rho = 0, \tag{1}$$

in which $q \in \mathcal{D}$, $\nabla^2 \phi(q,t)$ denotes the Laplacian of the scalar field $\phi(q,t) : \mathcal{D} \times \mathbb{R}_{\geq 0} \to \mathbb{R}_{>0}$,

$$\rho(p,q) = \begin{cases} 1 & \text{if } q = p_i, \ \forall i \in \mathcal{N} \\ 0 & \text{otherwise} \end{cases}, \tag{2}$$

$$\nu(\rho) = \begin{cases} \eta + \gamma & \text{if } \rho = 1 \\ \eta & \text{otherwise} \end{cases}, \tag{3}$$

and $\mu, \eta, \gamma \in \mathbb{R}_{>0}$, we extend (1) to characterize the heterogeneous prey model as a bounded and continuously differentiable density distribution $\phi(q,t)$ governed by

$$\frac{\partial \phi(q,t)}{\partial t} - \sum_{i \in \mathcal{N}} c_i(p,q,t) \cdot \nabla^2 \phi(q,t) + \sum_{i \in \mathcal{N}} h_i(p,q,t) = 0, \tag{4}$$

where the diffusivity $c_i(p,q,t) \in \mathbb{R}_{\geq 0}$ is defined as

$$c_i(p,q,t) = \begin{cases} \frac{c_d(t)}{N} + \lambda_i(t) & \text{if } q \in B_{d,i}(p_i, r_{d,i}) \\ \frac{c_d(t)}{N} & \text{otherwise} \end{cases}. \tag{5}$$

The diffusivity (5) incorporates the "scaring away" ability of Predator $i$, meaning that in addition to the prey's diffusion from its initial distribution with a speed of $c_d(t) : \mathbb{R}_{\geq 0} \to \mathbb{R}_{\geq 0}$, the prey inside the Euclidean ball $B_{d,i}(p_i, r_{d,i}) = \{q \in \mathcal{D} \mid \|q - p_i\| < r_{d,i}\}$ diffuse with a speed of $c_d(t) + \lambda_i(t)$, which characterizes the process of the prey being "scared away" by Predator $i$, where $\lambda_i(t) : \mathbb{R}_{\geq 0} \to \mathbb{R}$. The position of Predator $i$ is determined by the predator's dynamics which will be discussed in detail in Section III.

Note that the reason why $\lambda_i \in \mathbb{R}_{<0}$ is possible is that some types of predators in nature have evolved certain organs or behavioral techniques to lure prey, such as a deep-sea anglerfish using its esca, a luminescent organ, to lure fish swarm in dark environment [20].

The reaction term $h_i(p,q,t)$ in (4) is defined as

$$h_i(p,q,t) = \begin{cases} \frac{e_r(t)}{N} + f_{r,i}(q,t) & \text{if } q \in B_{r,i}(p_i, r_{r,i}) \\ \frac{e_r(t)}{N} & \text{otherwise} \end{cases}, \tag{6}$$

where $e_r(t) : \mathbb{R}_{\geq 0} \to \mathbb{R}_{\geq 0}$ characterizes how the prey are "consumed" by environmental factors, i.e., not by predators, assuming no interactions between how the environment affects the prey and how the predators affect the prey, and $f_{r,i}(q,t) : \mathcal{D} \times \mathbb{R}_{\geq 0} \to \mathbb{R}_{\geq 0}$ represents how the prey inside the ball $B_{r,i}(p_i, r_{r,i}) = \{q \in \mathcal{D} \mid \|q - p_i\| < r_{r,i}\}$ react to Predator $i$'s "consuming".

In summary, (4) incorporates four heterogeneous modalities: A) Diverse predator-prey interaction patterns, e.g., different predator has different eating habit, described by the heterogeneous reaction function $f_{r,i}(q,t)$, for any $i \in \mathcal{N}$; B) Predators' unequal consuming areas, e.g., different firefighting robot has different effective area, described by the radius $r_{r,i}$ of reaction area $B_{r,i}(p_i, r_{r,i})$; C) Predators' various "scaring away" abilities, meaning that the prey density in an circular area centered at different predator's location has different augmenting diffusion speed $\lambda_i(t)$; D) different predator has different "scaring away" area described by the radius $r_{d,i}$ of accelerated (corresponding to $\lambda_i(t) \in \mathbb{R}_{>0}$) or decelerated (corresponding to $\lambda_i(t) \in \mathbb{R}_{<0}$) diffusion area $B_{d,i}(p_i, r_{d,i})$. Note that we define the reaction area and the accelerated or decelerated diffusion area as Euclidean balls without loss of generality, and they do not necessarily have to be circular areas in practice.

The heterogeneous nature of the reaction-diffusion equation (4) allows one to specify numerous combinations of the four heterogeneity modalities for specific applications, for example: a) The process of marine predators preying on fish swarms can be portrayed by (4) with $n = 3$ and $e_r = 0$; b) Modelling herbivores eating plants, such as sparrows eating seeds and deer browsing on shrubs, e.g., [9], can be achieved by setting $n = 2$, $c_d = e_r = 0$ and $\lambda_i = 0, \forall i \in \mathcal{N}$; c) A team of robots monitoring eroded beach, coral reefs, or ocean floor can be described by (4) with $n = 2$, $c_d = 0$, and $\lambda_i = f_{r,i} = 0, \forall i \in \mathcal{N}$; d) A team of robots putting out ideally modeled wildfires, i.e., without fuel depletion and wind effect [17], can be governed by (4) with $n = 2$, $e_r = 0$ and $\lambda_i = 0, \forall i \in \mathcal{N}$. Among these examples, one can notice

that sometimes there exist interactions between predators' dynamics and prey's dynamics such as in cases a), b), and d), while sometimes only prey's dynamics affect predators' dynamics without the other way around such as in case c).

Note that in this section, we present some types of heterogeneities relevant to predators because they are closely related to the heterogeneous prey model (4) and hard to be separated, so in the next section, we only describe one more heterogeneity of the predator relevant to its dynamics.

## III. Heterogeneous Predator Model

A particular idea of cooperative hunting is that each individual in a team of predators cooperates with its neighbors such that the whole team spreads out across a domain to optimally cover the prey while eating the prey in the domain. Based on this idea, we consider four assumptions to design the predators' dynamics:

1) Each predator is in charge of a dominant subdomain of $\mathcal{D}$ in which all points are closer (with a certain distance metric) to the predator than any other predators, assuming the subdomains do not overlap and the union of all predators' dominant subdomains is equal to $\mathcal{D}$;
2) Different predator has different maximum translational speed and the larger the maximum speed a predator has, the larger its dominant subdomain should be;
3) Each predator acts only based on the local information of its neighboring predators and the prey within its dominant subdomain to ensure the decentralization of the scheme;
4) More predators should be in the area with higher density of prey and vice versa.

Inspired by [21], we consider the optimization problem

$$\min_p F(p,t) = \min_p \int_{\mathcal{D}} \min_{i\in\mathcal{N}} f(d(p_i(t),q))\phi(q,t)\,dq, \quad (7)$$

where $d(\cdot):\mathbb{R}^n\times\mathbb{R}^n\to\mathbb{R}_{\geq 0}$ is a distance metric in $\mathbb{R}^n$, and $f(\cdot):\mathbb{R}_{\geq 0}\to\mathbb{R}_{\geq 0}$ is defined as a smooth and monotonically increasing function because the prey closer to a predator in its dominant region are regarded as more effectively covered by that predator. Given a time instant $t$ and a configuration of the predators $p$, assuming $f(\cdot)=(\cdot)^2$, the optimization problem (7) can be rewritten as

$$\min_p F(p,t) = \min_p \sum_{i\in\mathcal{N}} \int_{\mathcal{V}_i(p)} d^2(p_i(t),q)\phi(q,t)\,dq, \quad (8)$$

where $\cup_{i\in\mathcal{N}}\mathcal{V}_i = \mathcal{D}$ can be the power diagram, multiplicatively weighted Voronoi diagram, or additively weighted Voronoi diagram, e.g., [22], to achieve Assumptions 1) and 2). We adopt the multiplicatively weighted Voronoi diagram because the additively weighted Voronoi diagram and the power diagram are sometimes not geometrically well-behaving, such as the predators not being inside their dominant regions or more than one predator being inside one Voronoi cell for the power diagram, and the disappearance of dominant regions for the additively weighted Voronoi diagram, as discussed in [22], if the additive weights or the relations between the additive weights and the positions of the predators are not carefully treated, which weakens the generality of the heterogeneity of the dominant regions or is even hard to achieve in such a dynamic environment considered in this paper. Thus, Predator $i$'s dominant region is defined as

$$\mathcal{V}_i(p) = \left\{ q\in\mathcal{D} \;\middle|\; \frac{\|p_i(t)-q\|}{v_i} \leq \frac{\|p_j(t)-q\|}{v_j}, \forall j\neq i \right\}, \quad (9)$$

where $i,j\in\mathcal{N}$, $v_i, v_j\in\mathbb{R}_{>0}$ are the maximum translational speeds of Predator $i$ and Predator $j$ respectively. One can notice that the distance metric utilized in (9) is $d(p_i(t),q) = \|p_i(t)-q\|/v_i, \forall i\in\mathcal{N}$. Thus the neighboring predators of Predator $i$ in Assumption 3) refer specifically to the Delaunay neighbors of Predator $i$.

The gradient of $F(p,t)$ with respect to $p_i$ is given when $n=2$ by [23]

$$\frac{\partial F(p,t)}{\partial p_i} = \frac{2}{v_i^2} m_i(p,t)(p_i - C_i(p,t))^T, \quad (10)$$

where $m_i(p,t)$ and $C_i(p,t)$ are defined as

$$m_i(p,t) = \int_{\mathcal{V}_i(p,t)} \phi(q,t)\,dq \quad (11)$$

and

$$C_i(p,t) = \frac{1}{m_i(p,t)} \int_{\mathcal{V}_i(p,t)} q\phi(q,t)\,dq, \quad (12)$$

respectively, which is a special case of the results in [24].

For the time-invariant density $\phi_i(q)$, assuming the single-integrator dynamics for each agent as

$$\dot{p}_i = u_i = -k_{p,i}\left(\frac{\partial F(p)}{\partial p_i}\right)^T, \quad (13)$$

where $k_{p,i}\in\mathbb{R}_{>0}$ is a proportional gain. The controller $u_i$ in (13) achieves Assumption 3) and is proved in [23] to asymptotically drive the system to converge to $p_i = C_i(p), \forall i\in\mathcal{N}$, in which configuration Assumption 4) is achieved. Note that although [23] focuses on the case of $n=2$, its conclusions also hold for $n\in\mathbb{Z}_+$.

For the time-varying prey density $\phi(q,t)$ governed by (4), if we adopt the controller (13) and choose the Lyapunov function as $L_1(p,t) = F(p,t) > 0$, utilizing the Reynolds transport theorem, e.g., [25], the total derivative of $L_1(p,t)$ with respect to time is calculated as

$$\begin{aligned}\frac{dL_1(p,t)}{dt} =& \sum_{i\in\mathcal{N}} \frac{-4k_{p,i}}{v_i^4} m_i^2(p,t)\|p_i - C_i(p,t)\|^2 \\ &+ \sum_{i\in\mathcal{N}} \int_{\mathcal{V}_i(p,t)} \frac{\|p_i-q\|^2}{v_i^2} \left( \sum_{i\in\mathcal{N}} c_i(p,q,t)\cdot \right. \\ &\left. \nabla^2\phi(q,t) - \sum_{i\in\mathcal{N}} h_i(p,q,t) \right) dq. \quad (14)\end{aligned}$$

Therefore, by LaSalle's invariance principle, a sufficient condition to ensure that $p_i$ asymptotically converges to

$C_i(p,t), \forall i \in \mathcal{N}$, is

$$\sum_{i\in\mathcal{N}} \int_{\mathcal{V}_i(p,t)} \frac{\|p_i - q\|^2}{v_i^2} \sum_{i\in\mathcal{N}} c_i(p,q,t)\cdot\nabla^2\phi(q,t)\,dq \leq \sum_{i\in\mathcal{N}} \int_{\mathcal{V}_i(p,t)} \frac{\|p_i - q\|^2}{v_i^2} \sum_{i\in\mathcal{N}} h_i(p,q,t)\,dq, \quad (15)$$

which can be intuitively explained by the requirement that the overall weighted diffusion process is "weaker" than the overall weighted reaction process in $\mathcal{D}$. However, this requirement, even a relaxation of (15) that the diffusion process is not much "stronger" than the reaction process, imposed on the prey's dynamics is still not tolerant enough such that the predators' dynamics should ideally be able to interact with any type of prey's dynamics while being stable.

One can notice from (10) that a critical point of $F(p,t)$ with respect to $p_i$ is $p_i(t) = C_i(p,t)$. In order to achieve and maintain $p_i(t) = C_i(p,t)$, similar to [26], [27], we analyze the Lyapunov function $L_2(p,t)$ defined as

$$L_2(p,t) = \sum_{i\in\mathcal{N}} \|p_i(t) - C_i(p,t)\|^2, \quad (16)$$

whose total derivative with respect to time is calculated as

$$\frac{dL_2(p,t)}{dt} = (p-C)^T \left( \left( I_{nN} - \frac{\partial C}{\partial p} \right) \dot{p} - \frac{\partial C}{\partial t} \right), \quad (17)$$

where $C = [C_1^T, C_2^T, \ldots, C_N^T]^T \in \mathbb{R}^{nN}$, and $I_{nN} \in \mathbb{R}^{nN\times nN}$ stands for the identity matrix of size $nN$. We omit some explicit arguments of the variables in (17) and the following content for notational convenience.

Analogous to [26], one way to enforce (17) to be negative definite is to let

$$\dot{p} = u = \left( I_{nN} - \frac{\partial C}{\partial p} \right)^{-1} \left( \kappa(C-p) + \frac{\partial C}{\partial t} \right), \quad (18)$$

where $u = [u_1^T, u_2^T, \ldots, u_N^T]^T \in \mathbb{R}^{nN}$ and $\kappa \in \mathbb{R}_{>0}$. Therefore, if the inverse term in (18) is well-defined, $p$ converges to $C$ as $t \to \infty$ with the rate of $exp(-\kappa t)$.

Employing the differentiation techniques presented in [25] and the analytical expression of the bisector between two Voronoi generators in terms of the multiplicatively weighted Voronoi partitioning presented in [22], the partial derivatives in (18) can be calculated as follows.

$$\frac{\partial C_i}{\partial p_i} = \frac{1}{m_i} \sum_{k\in\mathcal{N}_{\mathcal{V}_i}} \int_{\partial\mathcal{V}_{ik}} \frac{\frac{1}{v_i^2}(q-C_i)(q-p_i)^T\phi(q,t)}{\left\| \frac{1}{v_i^2}(q-p_i) - \frac{1}{v_k^2}(q-p_k) \right\|} dq, \quad (19)$$

for all $i \in \mathcal{N}$, where $\partial\mathcal{V}_{ik}$ and $\mathcal{N}_{\mathcal{V}_i}$ stand for the bisector between Voronoi cells $i$ and $k$ and the index set of the Delaunay neighbors of Predator $i$ in terms of the multiplicatively weighted Voronoi diagram, respectively. Likewise, $\frac{\partial C_i}{\partial p_j}$ can be calculated as

$$\frac{\partial C_i}{\partial p_j} = \frac{-1}{m_i} \int_{\partial\mathcal{V}_{ij}} \frac{\frac{1}{v_j^2}(q-C_i)(q-p_j)^T\phi(q,t)}{\left\| \frac{1}{v_j^2}(q-p_j) - \frac{1}{v_i^2}(q-p_i) \right\|} dq, \ \forall j \in \overline{\mathcal{N}_{\mathcal{V}_i}}, \quad (20)$$

where $\overline{\mathcal{N}_{\mathcal{V}_i}}$ stands for the set of indices of the closed neighborhood of Predator $i$ in the Delaunay graph. Note that $\partial\mathcal{V}_{ij}$ can appear to be discontinuous in $\mathcal{D}$ due to the properties of the multiplicatively weighted Voronoi diagram.

In addition, $\frac{\partial C_i}{\partial p_j} = 0, \forall j \notin \overline{\mathcal{N}_{\mathcal{V}_i}}$, and the partial derivative of $C(p,t)$ with respect to time $t$ is calculated as

$$\frac{\partial C_i}{\partial t} = \frac{1}{m_i} \int_{\mathcal{V}_i} (q - C_i) \left( \sum_{i\in\mathcal{N}} c_i(p,q,t)\cdot\nabla^2\phi(q,t) - \sum_{i\in\mathcal{N}} h_i(p,q,t) \right) dq. \quad (21)$$

However, the controller (18) does not meet Assumption 3) because the computation of the inverse term in (18) makes it centralized as it requires the information of all the predators. Nevertheless, Neumann series, e.g., [26], truncated after two entries can be adopted to approximate the inverse term in (18). Then, each predator's dynamics can be expressed as

$$\dot{p}_i = \frac{\partial C_i}{\partial t} + \kappa(C_i - p_i) + \sum_{j\in\overline{\mathcal{N}_{\mathcal{V}_i}}} \frac{\partial C_i}{\partial p_j} \left( \frac{\partial C_j}{\partial t} + \kappa(C_j - p_j) \right), \quad (22)$$

which is decentralized and scalable as the calculation of it only requires 1-hop adjacency information of Predator $i$, satisfying Assumption 3). Besides, another advantage is that the existence of the inverse term in (18) does not affect the validity of (22).

In summary, the heterogeneous predator dynamics (22) achieves Assumptions 1), 2), 3), and 4), and utilizing the proposed heterogeneous reaction-diffusion-based predator-prey interaction model (22) together with (4), various types of tasks can be accomplished with specifications of certain combinations of the five heterogeneous modalities considered in this scheme. In the next section, we will present a concrete example using the proposed predator-prey interaction scheme by specifying corresponding $n$, $N$, $c_d$, $\lambda_i$, $r_{d,i}$, $e_r$, $f_{r,i}$, $r_{r,i}$, and $v_i$, $\forall i \in \mathcal{N}$ in (4) and (22).

## IV. Experiment

In this section, we provide a concrete example by implementing the proposed scheme on $N = 10$ differential-drive wheeled robots at the Robotarium [28], where $\mathcal{D}$ is a rectangular domain with $x$-axis that ranges from $-1.6$ to $1.6$ and $y$-axis that ranges from $-1$ to $1$ as shown in Fig. 3, to demonstrate the scenario that a team of robots is deployed to put out ideally modeled wildfires. The single integrator dynamics developed in this paper corresponding to "carrier" points off and near the axles of the robots are linearly transformed to unicycle dynamics by the near-identity diffeomorphism [29] embedded in the Robotarium.

For this application, we assume no fire spread to the boundaries of the domain of interest $\mathcal{D}$ so zero Dirichlet boundary conditions are adopted. In fact, one can choose any combinations of Neumann boundary conditions and Dirichlet boundary conditions for particular application considerations, e.g., the domain of interest is enclosed by walls where fire can not pass through but the temperature on the

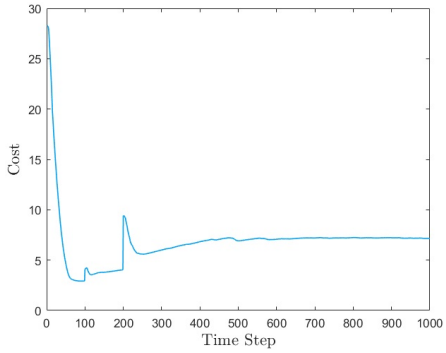


Fig. 2. Evolution of the cost $F(p,t)$ in (8).

boundaries can be non-zero, in which case the Neumann boundary conditions should be applied. Also, since the robots do not "scare away" the fire, the relative augmenting diffusion speeds are set to be $\lambda_i = 0, \forall i \in \mathcal{N}$. The natural diffusion speed of fire is set to be $c_d = 1$, and the natural reaction pattern of fire is set to be $e_r = 0$. The reaction function is set to be $f_{r,i} = \sigma_i \phi(q,t)$, $\forall i \in \mathcal{N}$, where $\sigma_i$ among the 10 robots are collected in the vector $\sigma = 10 \cdot [20, 16, 12, 8, 12, 16, 20, 16, 12, 8]^T$, and likewise, the predators' reaction radii are specified as $r_r = 0.0143 \cdot [4, 5, 6, 7, 7, 7, 7, 6, 5, 4]^T$. Note that normally the prey density should not be negative so the reaction function should be chosen such that $\phi(q,t) \in \mathbb{R}_{>0}, \forall q \in \mathcal{D}, t \in \mathbb{R}_{\geq 0}$. However, if the density represents the temperature and certain sorts of extinguishing agents can cause sub-zero temperatures, then it is reasonable to choose $f_{r,i}$ that can induce $\phi(q,t) \in \mathbb{R}_{<0}$, but what should be avoided is that $m_i(p,t) = 0, \forall i \in \mathcal{N}$ for validity of (19), (20), and (21). Additionally, the maximum speeds among the 10 robots are put in the vector $v = [6, 7, 8, 9, 9, 8, 7, 6, 5, 5]^T$, and $u_i = MIN\,(v_i, \|u_i\|) \cdot u_i / \|u_i\|$. Note that $v$ reflects the relative maximum translational speeds among the predators, so it can be scaled by constant factors without affecting the geometry of the predators' region of dominance. The initial positions of the 10 robots are as shown in Fig. 3(a).

The initial wildfire density at time step 1 is set to be an unnormalized Gaussian distribution with the mean as $\mu_0 = [-0.6, -0.1]^T$ and covariance matrix as $\Sigma_0 = 0.0625 I_2$ as shown in Fig. 3(a), and there are two more spot fires ignited by firebrands or arsonists at time steps 100 and 200 with their means as $\mu_1 = [-0.2, -0.3]^T$ and $\mu_2 = [0.2, -0.2]^T$, and covariance matrices as $\Sigma_1 = 0.0004 I_2$ and $\Sigma_2 = 0.0009 I_2$, as shown in Fig. 3(c) and Fig. 3(e), respectively.

The robots in Fig. 3 are labeled with index numbers with different colors for distinguishment of them, and the colored dots are the centers of mass $C_i(p,t)$ of corresponding Voronoi cells. One can notice that the robots gradually achieve and then maintain the time-varying locally optimal configuration, i.e., centroidal Voronoi tessellation [30], while putting out the wildfire as the time approaches.

The evolution of the cost $F(p,t)$ is shown in Fig. 2, where one can notice that there are two jumps at time steps 100 and 200 due to the introduction of new spot fires. After each jump, the cost first decreases due to the stronger effect of the robots' approaching their centers of mass than the effect of the diffusion of the density, and then increases due to the effect of the diffusion of the density while the robots are maintaining at their centers of mass, where the increasing speed overall decreases due to the effect of consumption of the density by the reaction process.

## V. Conclusion

In this paper, we investigated a heterogeneous predator-prey interaction scheme using the time-varying coverage controller with multiplicatively weighted Voronoi cells driven by reaction-diffusion processes, where the predators and prey are modeled as individual agents and space-time dependent densities, respectively. Diverse tasks can be accomplished benefiting from the scheme formulation considering five heterogeneous modalities. The effectiveness of the proposed scheme is demonstrated through an experiment performed on a team of robots with specific heterogeneous settings.

## Acknowledgment

The authors thank Soobum Kim for the help with numerical calculations of multiplicatively weighted Voronoi cells, and Tirtha Banerjee for discussions on wildfire models.

## References

[1] M. Haque, A. Rahmani, and M. Egerstedt, "Geometric foraging strategies in multi-agent systems based on biological models," in *49th IEEE Conference on Decision and Control (CDC)*. IEEE, 2010, pp. 6040–6045.

[2] P. N. Newton, "Associations between langur monkeys (presbytis entellus) and chital deer (axis axis): chance encounters or a mutualism?" *Ethology*, vol. 83, no. 2, pp. 89–120, 1989.

[3] M. Y. Arafat and S. Moh, "Bio-inspired approaches for energy-efficient localization and clustering in uav networks for monitoring wildfires in remote areas," *IEEE Access*, vol. 9, pp. 18 649–18 669, 2021.

[4] J. D. Madden, R. C. Arkin, and D. R. MacNulty, "Multi-robot system based on model of wolf hunting behavior to emulate wolf and elk interactions," in *2010 IEEE International Conference on Robotics and Biomimetics*. IEEE, 2010, pp. 1043–1050.

[5] M. A. Haque, A. R. Rahmani, and M. B. Egerstedt, "Biologically inspired confinement of multi-robot systems," *International Journal of Bio-Inspired Computation*, vol. 3, no. 4, pp. 213–224, 2011.

[6] J.-P. de la Croix and M. Egerstedt, "Group-size selection for a parameterized class of predator-prey models." Georgia Institute of Technology, 2014.

[7] A. Prorok, M. Malencia, L. Carlone, G. S. Sukhatme, B. M. Sadler, and V. Kumar, "Beyond robustness: A taxonomy of approaches towards resilient multi-robot systems," *arXiv preprint arXiv:2109.12343*, 2021.

[8] R. Lin and M. Egerstedt, "Dynamic multi-target tracking using heterogeneous coverage control," in *2023 IEEE/RSJ International Conference on Intelligent Robots and Systems (IROS)*, Detroit, MI, Oct. 2023.

[9] M. Egerstedt, *Robot Ecology: Constraint-Based Design for Long-Duration Autonomy*. Princeton University Press, 2021.

[10] R. Isaacs, *Differential games: a mathematical theory with applications to warfare and pursuit, control and optimization*. Courier Corporation, 1999.

[11] I. M. Mitchell, A. M. Bayen, and C. J. Tomlin, "A time-dependent hamilton-jacobi formulation of reachable sets for continuous dynamic games," *IEEE Transactions on automatic control*, vol. 50, no. 7, pp. 947–957, 2005.

[12] H. Huang, J. Ding, W. Zhang, and C. J. Tomlin, "A differential game approach to planning in adversarial scenarios: A case study on capture-the-flag," in *2011 IEEE International Conference on Robotics and Automation*. IEEE, 2011, pp. 1451–1456.

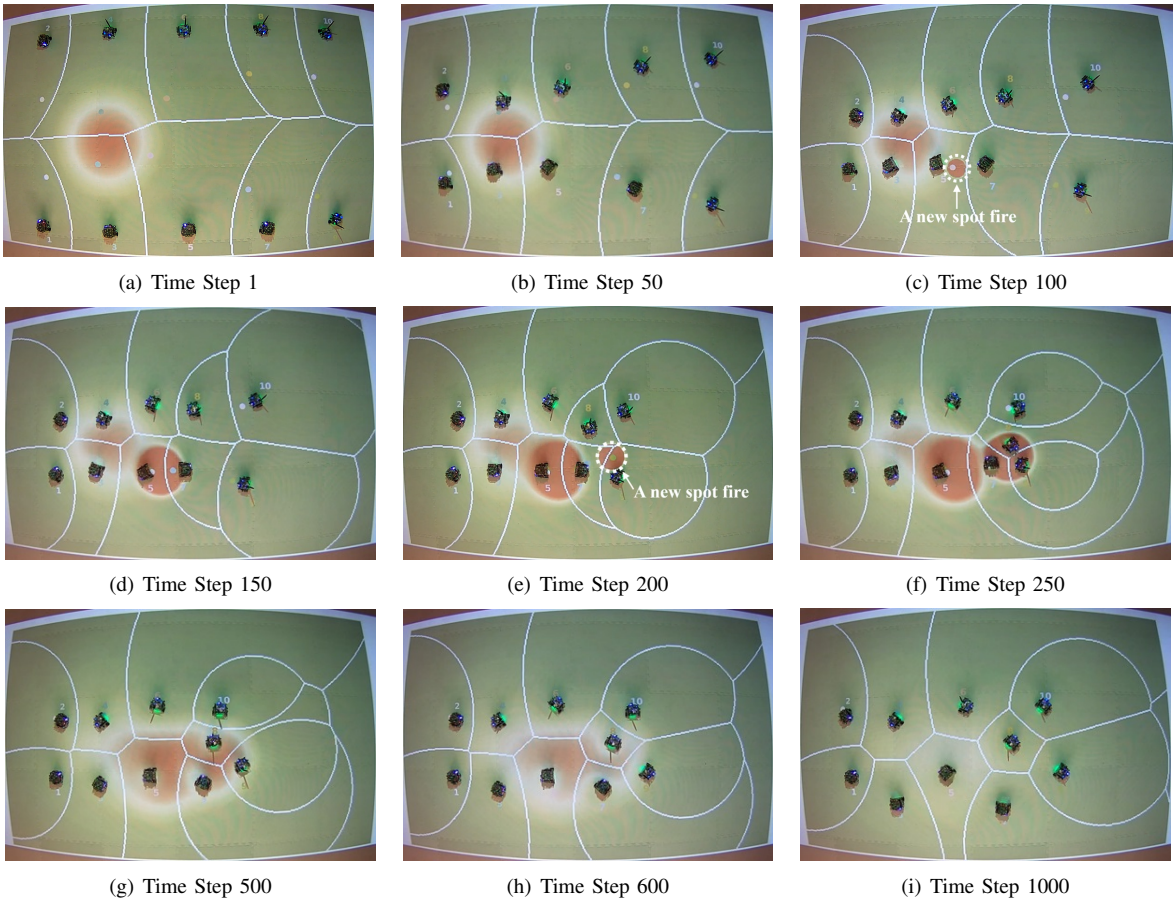


(a) Time Step 1 (b) Time Step 50 (c) Time Step 100

(d) Time Step 150 (e) Time Step 200 (f) Time Step 250

(g) Time Step 500 (h) Time Step 600 (i) Time Step 1000

Fig. 3. Deploying a team of 10 differential-drive wheeled robots, to put out ideally modeled wildfires represented by the densities on the Robotarium, with the red area representing high density and the green area representing low density. The colored dots represent a locally optimal configuration of the robots that are indexed by corresponding colored numbers. Each robot is in charge of a region of dominance with a set of white curves as its boundaries.


[13] Z. Zhou, W. Zhang, J. Ding, H. Huang, D. M. Stipanović, and C. J. Tomlin, "Cooperative pursuit with voronoi partitions," *Automatica*, vol. 72, pp. 64–72, 2016.

[14] A. Pierson, Z. Wang, and M. Schwager, "Intercepting rogue robots: An algorithm for capturing multiple evaders with multiple pursuers," *IEEE Robotics and Automation Letters*, vol. 2, no. 2, pp. 530–537, 2016.

[15] S.-Y. Liu and K. Hedrick, "The application of domain of danger in autonomous agent team and its effect on exploration efficiency," in *Proceedings of the 2011 American Control Conference*. IEEE, 2011, pp. 4111–4116.

[16] J. Neira, C. Sequeiros, R. Huamani, E. Machaca, P. Fonseca, and W. Nina, "Review on unmanned underwater robotics, structure designs, materials, sensors, actuators, and navigation control," *Journal of Robotics*, vol. 2021, pp. 1–26, 2021.

[17] J. Mandel, L. S. Bennethum, J. D. Beezley, J. L. Coen, C. C. Douglas, M. Kim, and A. Vodacek, "A wildland fire model with data assimilation," *Mathematics and Computers in Simulation*, vol. 79, no. 3, pp. 584–606, 2008.

[18] M. Haque, A. Rahmani, M. Egerstedt, and A. Yezzi, "Efficient foraging strategies in multi-agent systems through curve evolutions," *IEEE Transactions on Automatic Control*, vol. 59, no. 4, pp. 1036–1041, 2013.

[19] J. D. Murray, *Mathematical biology: I. An introduction*. Springer, 2002.

[20] P. J. Herring and O. Munk, "The escal light gland of the deep-sea anglerfish haplophryne mollis (pisces: Ceratioidei) with observations on luminescence control," *journal of the Marine Biological Association of the United Kingdom*, vol. 74, no. 4, pp. 747–763, 1994.

[21] J. Cortes, S. Martinez, T. Karatas, and F. Bullo, "Coverage control for mobile sensing networks," *IEEE Transactions on robotics and Automation*, vol. 20, no. 2, pp. 243–255, 2004.

[22] B. Boots, K. Sugihara, S. N. Chiu, and A. Okabe, "Spatial tessellations: concepts and applications of voronoi diagrams," 2009.

[23] S. Kim, M. Santos, L. Guerrero-Bonilla, A. Yezzi, and M. Egerstedt, "Coverage control of mobile robots with different maximum speeds for time-sensitive applications," *IEEE Robotics and Automation Letters*, vol. 7, no. 2, pp. 3001–3007, 2022.

[24] R. Lin and M. Egerstedt, "Coverage control on the special euclidean groups," in *2023 American Control Conference (ACC)*. IEEE, 2023, pp. 1972–1979.

[25] R. Niven, L. Cordier, E. Kaiser, M. Schlegel, and B. Noack, "New conservation laws based on generalised reynolds transport theorems," in *22nd Australasian Fluid Mechanics Conference AFMC2020*, 2020.

[26] S. G. Lee, Y. Diaz-Mercado, and M. Egerstedt, "Multirobot control using time-varying density functions," *IEEE Transactions on robotics*, vol. 31, no. 2, pp. 489–493, 2015.

[27] J. Cortés and M. Egerstedt, "Coordinated control of multi-robot systems: A survey," *SICE Journal of Control, Measurement, and System Integration*, vol. 10, no. 6, pp. 495–503, 2017.

[28] S. Wilson, P. Glotfelter, L. Wang, S. Mayya, G. Notomista, M. Mote, and M. Egerstedt, "The robotarium: Globally impactful opportunities, challenges, and lessons learned in remote-access, distributed control of multirobot systems," *IEEE Control Systems Magazine*, vol. 40, no. 1, pp. 26–44, 2020.

[29] R. Olfati-Saber, "Near-identity diffeomorphisms and exponential e-tracking and 6-stabilization of first-order nonholonomic se (2) vehicles," *Proceeding of the 2002 ACC*, 2002.

[30] Q. Du, V. Faber, and M. Gunzburger, "Centroidal voronoi tessellations: Applications and algorithms," *SIAM review*, vol. 41, no. 4, pp. 637–676, 1999.